Torque-coupling and particle–turbulence interactions

Helge I. Andersson, Lihao Zhao and Mustafa Barri

Journal of Fluid Mechanics / Volume 696 / April 2012, pp 319 - 329
DOI: 10.1017/jfm.2012.44, Published online: 28 February 2012

J. Fluid Mech. (2012), *vol.* 696, *pp.* 319–329.
doi:10.1017/jfm.2012.44

Torque-coupling and particle–turbulence interactions

Helge I. Andersson†, Lihao Zhao and Mustafa Barri

Department of Energy and Process Engineering, The Norwegian University of Science and Technology, NO-7491 Trondheim, Norway

(Received 6 November 2011; revised 13 January 2012; accepted 22 January 2012; first published online 28 February 2012)

A novel scheme for strong coupling between inertial Lagrangian point particles and a continuous Eulerian fluid phase has been developed. A full mechanical coupling can only be achieved if torque-coupling is applied along with the more conventional force-coupling. The torque vector acting from the particles on the fluid is expressed in terms of a new antisymmetric particle stress tensor which adds to the Stokes stress tensor. A strongly-coupled simulation of a turbulent channel flow laden with prolate spheroidal particles with aspect ratio 5:1 demonstrated that the inclusion of torque-coupling reduced the modulation of the turbulent flow field observed in a two-way force-coupled simulation. The spin and orientation of the spheroids were significantly affected.

Key words: particle/fluid flow, suspensions, turbulence simulation

1. Introduction

The motion of small heavy particles embedded in a turbulent carrier fluid is of vital importance in industrial and environmental fluid mechanics. The dynamics of inertial particles suspended in a fluid flow constitute a many-body dynamical problem intricately coupled with a continuum flow problem. A viable approach would therefore be to represent both the fluid flow and the particle motion in accordance with the basic laws of mechanics, i.e. so-called 'first principles'. The flow field is thus obtained directly from the Navier–Stokes equations in a direct numerical simulation (DNS) while the particle dynamics is governed by equations of translational and rotational motion for each and every particle.

The Lagrangian point-particle approach has been used extensively in turbulent dispersed multiphase flow computations. For several decades such one-way coupled simulations have been performed with the view to study particle dispersion, transport and deposition; see e.g. the recent review by Balachandar & Eaton (2010). In certain parameter ranges, however, the presence of solid particles in the fluid may alter the flow field and two-way coupled simulations (Eaton 2009) are required in order to investigate the turbulence modulation caused by inertial particles. Such simulations became feasible about two decades ago (e.g. Squires & Eaton 1990) and are today performed with several million spherical point particles (Zhao, Andersson & Gillissen 2010; Zhao & Andersson 2011).

† Email address for correspondence: helge.i.andersson@ntnu.no

The point-particle approach is based on the assumption that the particle diameter d is smaller than the Kolmogorov length scale η and the particle Reynolds number $Re_p < 1$. For finite-size particles, i.e. $d > \eta$, the flow field in the vicinity of each particle has to be resolved numerically. Uhlmann (2008) and Lucci, Ferrante & Elghobashi (2010) used an immersed boundary method (IBM) to achieve this goal for as many as 4096 and 6400 finite-size freely moving spherical particles, respectively. In such fully-resolved approaches, the boundary conditions imposed on each individual particle surface automatically ensure both force- and torque-coupling between the particles and the fluid.

Both the point-particle and the fully-resolved approaches are also applicable to non-spherical particles. Here, we are concerned with the former, which was extended to ellipsoidal particles by Zhang *et al.* (2001). That study, as well as the subsequent investigations by Mortensen *et al.* (2008) and Marchioli, Fantoni & Soldati (2010) were confined only to one-way coupling. If, on the other hand, the feedback from the suspended particles is of concern, one may conjecture that not only force-coupling but also torque-coupling might be important. To the authors' knowledge, no such scheme is available for point particles.

In the present paper a novel scheme for torque-coupling is presented which enables for the first time a strong mechanical coupling between inertial point particles and the Newtonian carrier fluid. To this end a particle stress tensor is introduced into the particle-laden Navier–Stokes equations which, analogously to the stress tensor for micropolar fluids (Eringen 1966), is proportional to the rotational slip velocity. Results from a strongly-coupled simulation of elongated particles are presented with the view to illustrate the significance of the new scheme.

2. A novel scheme for strong two-way coupling

Dilute suspensions of solid point particles in a viscous (Newtonian) fluid are routinely treated in a mixed Lagrangian–Eulerian approach in which the particle motion is modelled in a Lagrangian way and the fluid flow is formulated in an Eulerian framework, e.g. by means of DNS. Two-way coupled simulations imply that the fluid motion is affected by forces from the point particles (Eaton 2009), but the fluid is unaffected by the particle torques. To this end a new scheme aimed also to allow for torque-coupling between the inertial particles and the flow field is devised. Prolate spheroids are used as a prototype of elongated fibre-like particles to demonstrate the performance of the scheme. Effects of gravity on the particle dynamics and the fluid motion are neglected.

2.1. *Particle dynamics*

Let us consider the motion of ellipsoidal particles in a Newtonian fluid with density ρ and dynamic coefficient of viscosity μ. More specifically, the particles are prolate spheroids with mass m and aspect ratio $\lambda = b/a$ where a and b are the semi-minor and semi-major axes, respectively. The mathematical modelling of the ellipsoidal point particles follows the methodology outlined by Zhang *et al.* (2001) and subsequently adopted by Mortensen *et al.* (2008) and Marchioli *et al.* (2010). The translational and rotational motion of one single particle is governed by:

$$m\,\frac{\mathrm{d}v_i}{\mathrm{d}t} = F_i, \tag{2.1a}$$

$$I'_{ij}\,\frac{\mathrm{d}\omega'_j}{\mathrm{d}t} + \epsilon_{ijk}\omega'_j I'_{kl}\omega'_l = N'_i \tag{2.1b}$$

respectively, where ϵ_{ijk} is the Levi-Civita alternating or permutation tensor. Two different Cartesian frames of reference are used. Newton's second law of motion (2.1*a*) is expressed in an inertial frame $x_i = \langle x_1, x_2, x_3 \rangle$ and Euler's equation (2.1*b*) is formulated in the particle frame $x'_i = \langle x'_1, x'_2, x'_3 \rangle$ with its origin at the particle mass centre and the coordinate axes aligned with the principal directions of inertia. Thus, $v_i = \mathrm{d}x_i/\mathrm{d}t$ denotes the translational particle velocity in the inertial frame whereas ω'_i is the angular velocity of the particle in the particle frame and I'_{ij} is the moment of inertia tensor for the non-spherical particles.

If the particles are sufficiently small so that the neighbouring flow can be considered as Stokesian, the force F_i acting on a particle from the surrounding fluid can be expressed as:

$$F_i = D_{ij}(u_j - v_j) + \frac{Re_\kappa^{1/2}}{\mu a} D_{ij} L_{jk} D_{kl}(u_l - v_l), \quad D_{ij} = \pi \mu a K_{ij}, \tag{2.2}$$

where u_i is the fluid velocity at the particle position and $Re_\kappa = \rho \kappa a^2/\mu$ is a shear Reynolds number based on the modulus κ of the velocity gradient tensor. Here, L_{ij} is the lift tensor and the resistance tensor K_{ij} in the inertial frame is related to the resistance tensor K'_{ij} in the particle frame as $K_{ij} = A^t_{ik} K'_{kl} A_{lj}$ where A_{ij} denotes the orthogonal transformation matrix which relates the same vector in the two different frames through the linear transformation $x_i = A_{ij} x'_j$. The expressions for the hydrodynamic drag and lift forces on a non-spherical particle were derived by Brenner (1964) and Harper & Chang (1968), respectively. According to (2.2), which is valid only when the particle Reynolds number is low, the force acting on the particle is therefore linearly dependent on the difference in translational velocity between the fluid and the particle.

Similarly, the torque N'_i is linearly dependent on the difference in angular velocity between the fluid and the particle, i.e.

$$N'_1 = \frac{16\pi\mu a^3 \lambda}{3(\beta_0 + \lambda^2 \gamma_0)} [(1 - \lambda^2) S'_{23} + (1 + \lambda^2)(\Omega'_1 - \omega'_1)], \tag{2.3a}$$

$$N'_2 = \frac{16\pi\mu a^3 \lambda}{3(\alpha_0 + \lambda^2 \gamma_0)} [(\lambda^2 - 1) S'_{13} + (1 + \lambda^2)(\Omega'_2 - \omega'_2)], \tag{2.3b}$$

$$N'_3 = \frac{32\pi\mu a^3 \lambda}{3(\alpha_0 + \beta_0)} (\Omega'_3 - \omega'_3). \tag{2.3c}$$

The parameters α_0, β_0 and γ_0 depend on the particle aspect ratio λ. These expressions were first derived by Jeffery (1922) for an ellipsoidal particle in creeping motion, i.e. $Re_p < 1$. Here, S'_{ij} and Ω'_i denote the fluid rate-of-strain tensor and rate-of-rotation vector, respectively. The vorticity of the fluid flow field is thus $2\Omega'_i$.

The shape of a prolate spheroid is characterized by the particle aspect ratio λ, whereas the ability of the particle to adjust to the ambient flow field can be estimated in terms of the particle response time:

$$\tau = \frac{2\lambda \rho_p a^2}{9\mu} \frac{\ln(\lambda + \sqrt{\lambda^2 - 1})}{\sqrt{\lambda^2 - 1}} \tag{2.4}$$

where ρ_p is the particle density. The response time τ was introduced by Zhang *et al.* (2001) as a time scale of the translational motion. The rotational relaxation time for spherical particles is $3\tau/10$ (Zhao & Andersson 2011), but no such scalar time scale seems to exist for non-spherical particles (Mortensen *et al.* 2008).

2.2. *Strong two-way coupling*

Cauchy's equation of motion, i.e. the principle of conservation of linear momentum, can be expressed in Cartesian tensor notation as:

$$\rho \frac{\mathrm{D}u_i}{\mathrm{D}t} = \frac{\partial T_{ji}}{\partial x_j} + \rho f_i \tag{2.5}$$

where T_{ji} is a stress tensor and f_i is a body force. For a Newtonian fluid the stress tensor is:

$$T_{ji} = T_{ij} = -p\delta_{ij} + \mu \left(\frac{\partial u_i}{\partial x_j} + \frac{\partial u_j}{\partial x_i} \right) \tag{2.6}$$

and when this symmetric stress tensor is inserted in the Cauchy equation (2.5) we arrive at the celebrated Navier–Stokes equations.

The force from an individual particle on the fluid is equal to $-F_i$ according to Newton's third law *'actio equals reactio'*. The feedback from n_p particles within a given volume Δ (e.g. a grid cell) adds up to:

$$f_i^P = -\frac{1}{\Delta} \sum_{l=1}^{n_p} F_i \tag{2.7}$$

where F_i is given by (2.2). This force per unit volume can be included in the linear momentum equation (2.5) to account for the effect of the solid particles on the fluid motion. This is known as the *point-force approximation* to two-way coupling; see e.g. Balachandar & Eaton (2010). This approach was probably first introduced by Squires & Eaton (1990) in order to study the modulation of isotropic turbulence by spherical particles.

Similarly, the torque from a single particle on the fluid is $-N_i$ where N_i is given in second (2.3). It is known from tensor analysis that to any vector $-N_i$ there corresponds an antisymmetric tensor of second order that contains the same information as the vector; see e.g. Irgens (2008). The torque vector $-N_i$ can thus be obtained from a particle stress tensor T_{ij}^P according to:

$$-N_m = -\tfrac{1}{2}\epsilon_{mij} T_{ij}^P \Delta. \tag{2.8}$$

In practice, the torque should be the sum of torques over all particles inside the grid cell under consideration. We furthermore assume that $T_{ij}^P = -T_{ji}^P$, i.e. we impose an antisymmetry on T_{ij}^P. From (2.8) we thus arrive at the following expression for the anti-symmetric particle stress tensor:

$$T_{ij}^P = \frac{1}{\Delta} \sum_{l=1}^{n_p} \epsilon_{mij} N_m = \frac{1}{\Delta} \sum_{l=1}^{n_p} \begin{bmatrix} 0 & +N_3 & -N_2 \\ -N_3 & 0 & +N_1 \\ +N_2 & -N_1 & 0 \end{bmatrix} \tag{2.9}$$

where the summation is carried out over all particles in the volume Δ.

When the new stress tensor (2.9) is introduced in the Cauchy equation (2.5) together with the familiar Stokes stress tensor (2.6), the torques exerted by the particles on the fluid give rise to the additional term:

$$\frac{\partial T_{ji}^P}{\partial x_j} = -\frac{\partial T_{ij}^P}{\partial x_j} = -\frac{1}{\Delta} \epsilon_{mij} \frac{\partial}{\partial x_j} \sum_{l=1}^{n_p} N_m \tag{2.10}$$

to be added to the x_i-component of the Navier–Stokes equation. If Δ is the volume of a computational grid cell, this accounts for the feedback on the fluid of the total torque from the n_p particles inside the cell. This is a point-torque approximation analogous to the point-force approximation (2.7) commonly employed in two-way coupled simulations.

2.3. *Analogy with micropolar fluids*

For micropolar fluids Eringen (1966) suggested that Stokes' stress tensor (2.6) should be replaced by:

$$T_{ij} = -p\delta_{ij} + \mu\left(\frac{\partial u_i}{\partial x_j} + \frac{\partial u_j}{\partial x_i}\right) + \mu_r\left(\frac{\partial u_j}{\partial x_i} - \frac{\partial u_i}{\partial x_j}\right) - 2\mu_r\epsilon_{mij}\omega_m. \tag{2.11}$$

The positive constant μ_r is called the dynamic *microrotation viscosity* and this new viscosity coefficient is understood to be a fluid property which is characteristic for the fluid–particle suspension. A comprehensive account of the theory of micropolar fluids has been provided by Łukaszewicz (1999).

The expression within the second parenthesis in (2.11) is directly related to the angular velocity of the fluid as:

$$\left(\frac{\partial u_j}{\partial x_i} - \frac{\partial u_i}{\partial x_j}\right) = 2\Omega_m\epsilon_{mij} \tag{2.12}$$

since components of the fluid angular velocity vector can be written as $\Omega_m = (1/2)\epsilon_{mji}\partial u_i/\partial x_j$ and use has been made of the identity $\epsilon_{ijk}\epsilon_{rsk} = \delta_{ir}\delta_{js} - \delta_{is}\delta_{jr}$. Eringen's expression (2.11) for the stress tensor in a micropolar fluid can now be rewritten as:

$$T_{ij} = -p\delta_{ij} + \mu\left(\frac{\partial u_i}{\partial x_j} + \frac{\partial u_j}{\partial x_i}\right) + \underbrace{2\mu_r\epsilon_{mij}(\Omega_m - \omega_m)}_{T^P_{ij}} \tag{2.13}$$

where the last term is considered to represent the effect of the particles on the motion of the fluid–particle mixture. The vector field ω_i is called the field of *microrotation* and represents the angular velocity of the solid particles. In the theory for micropolar fluids ω_i is obtained from a transport equation for angular momentum; see Eringen (1966) and Łukaszewicz (1999). In the present context, however, the expression (2.9) replaces the modelling of T^P_{ij} (2.13) used in the continuum mechanics approach by Eringen (1966). The concept of microrotation viscosity μ_r is therefore avoided since the particle stress tensor is computed directly from the individual point particles inside a fluid volume (or grid cell) in accordance with (2.9).

3. Particle-laden channel flow simulation with force- and torque-coupling

A particle-laden fully-developed turbulent channel flow at Reynolds number $Re = 360$ based on the channel height h and the wall-friction velocity u_* is now considered. The Eulerian flow field u_i of the carrier phase is obtained by means of DNS, i.e. by solving the Cauchy equation (2.5) in time and three-dimensional space. The DNS-solver is the same as that used by Mortensen *et al.* (2008) for one-way coupled simulations, but now with the point-force and the point-torque approximations in (2.7) and (2.10) implemented. Zhang *et al.* (2001) assumed that an ellipsoidal particle is deposited on the wall if the particle touches the surface. In the present study, however, we follow Mortensen *et al.* (2008) and assume that a particle which hits

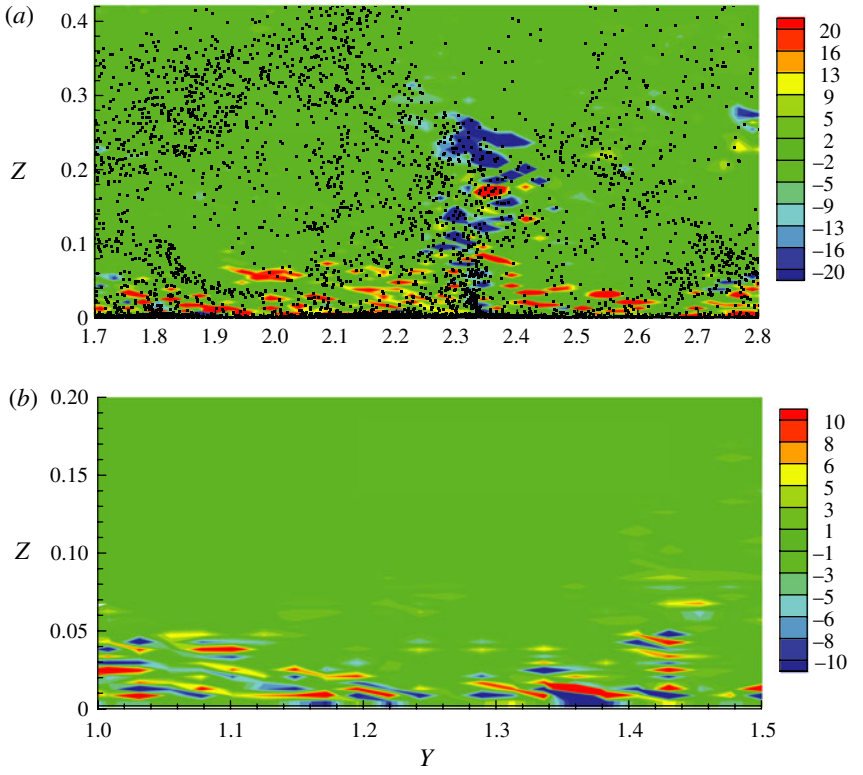

FIGURE 1. Instantaneous feedback in the streamwise direction from the spheroidal particles on the flow field. Near-wall contour plots in the cross-sectional plane of: (*a*) particle force f_x^P; and (*b*) the torque force $\partial T_{jx}^P/\partial x_j$. The coordinates Y and Z in the spanwise and wall-normal directions, respectively, are scaled with h and $Z = 0.1$ corresponds to $z^+ = 36$.

the wall bounces elastically back into the flow while retaining its translational velocity in the homogeneous directions as well as its spin. The computational domain is $6h$ and $3h$ in the streamwise and spanwise directions, respectively, and the computational mesh consists of 128^3 grid points.

Two and a half million mono-sized non-spherical particles are released randomly into an already developed turbulent flow field. The particles are prolate spheroids with aspect ratio $\lambda = 5$ and particle response time τ^+ equal to 30. The superscript $+$ indicates that τ in (2.4) is normalized with the viscous time scale ν/u_*^2. The temporal sampling interval Δt^+ is 3600 and statistics averaged also in the two homogeneous directions are denoted by angular brackets.

To enable an investigation of the influence of torque-coupling in addition to force-coupling alone, we also performed another simulation with the same spheroidal particles in the same channel but only with the point-force approximation (2.7) activated. To the best of our knowledge, no such two-way coupled simulations with non-spherical point particles have been performed previously. We are thus in the position to compare results from a *strongly-coupled* (i.e. force- and torque-coupling) with a *weakly-coupled* (only force-coupling) simulation.

It is well-known that inertial particles concentrate preferentially in a turbulent flow field; see e.g. Balachandar & Eaton (2010). This is reflected in figure 1 which shows

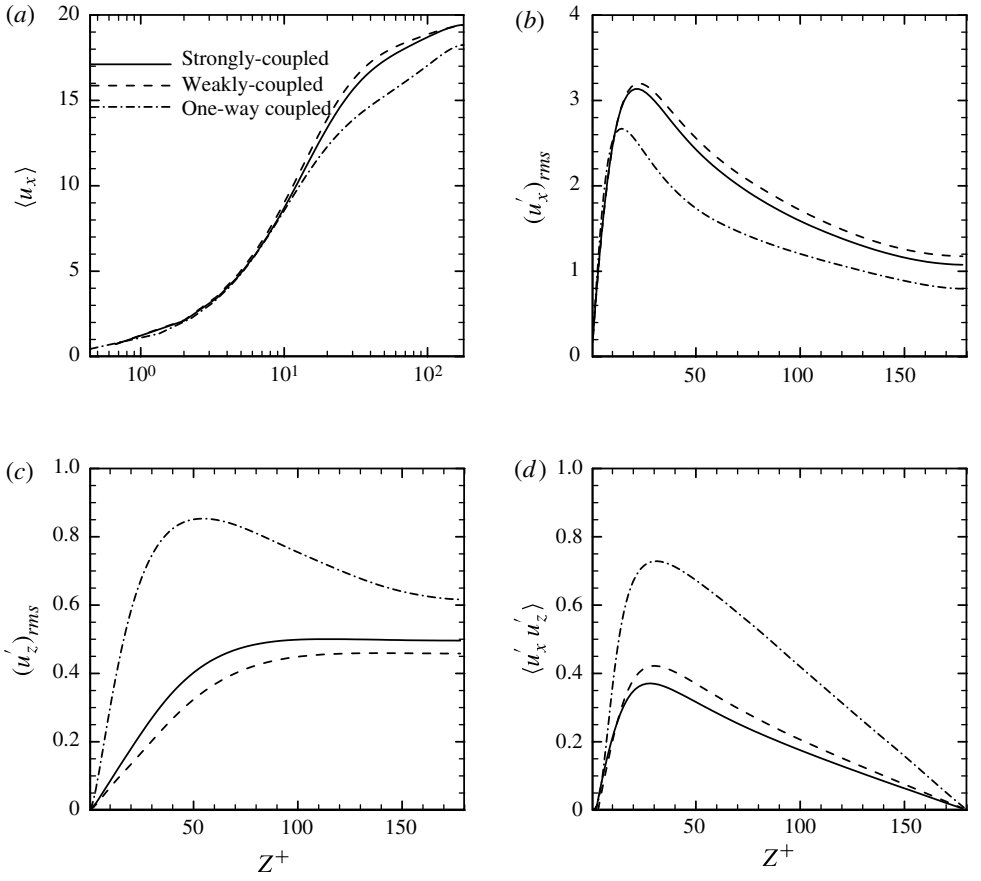

FIGURE 2. Flow-field statistics from the strongly-coupled simulation (solid lines) compared with results from the weakly-coupled simulation (broken lines). Results from a one-way coupled simulation (dash-dotted lines) are included for comparative purposes: (*a*) mean streamwise velocity $\langle u_x \rangle$; (*b*) streamwise turbulence intensity $(u_x')_{rms}$; (*c*) wall-normal turbulence intensity $(u_z')_{rms}$; (*d*) Reynolds shear stress $\langle u_x' u_z' \rangle$.

the cross-sectional distribution of the instantaneous feedback from the inertial point particles on the fluid. It is readily seen that the streamwise component f_x^P attains appreciable values not only in the immediate vicinity of the wall but also out in the logarithmic wall layer, i.e. beyond $z^+ = 30$. On the contrary, the streamwise component of $\partial T_{ji}^P / \partial x_j$ makes a significant contribution only for $Z < 0.05$, i.e. in the viscous-dominated sublayer. Besides the spotty appearance of the particle force and the torque force, it is noteworthy that the latter attains locally high values which are comparable in magnitude with the local particle-force values.

The primary fluid statistics are presented in figure 2. The two-way force-coupling gives rise to a substantially increased mean velocity $\langle u_x \rangle$ and streamwise turbulence intensity $(u_x')_{rms}$ while the two other turbulence intensities and the Reynolds shear stress $\langle u_x' u_z' \rangle$ are damped compared with the one-way coupled channel flow. Exactly the same effects were reported from our recent study on spherical particles (Zhao *et al.* 2010). The tendencies observed with force-coupling alone are reduced in the force-

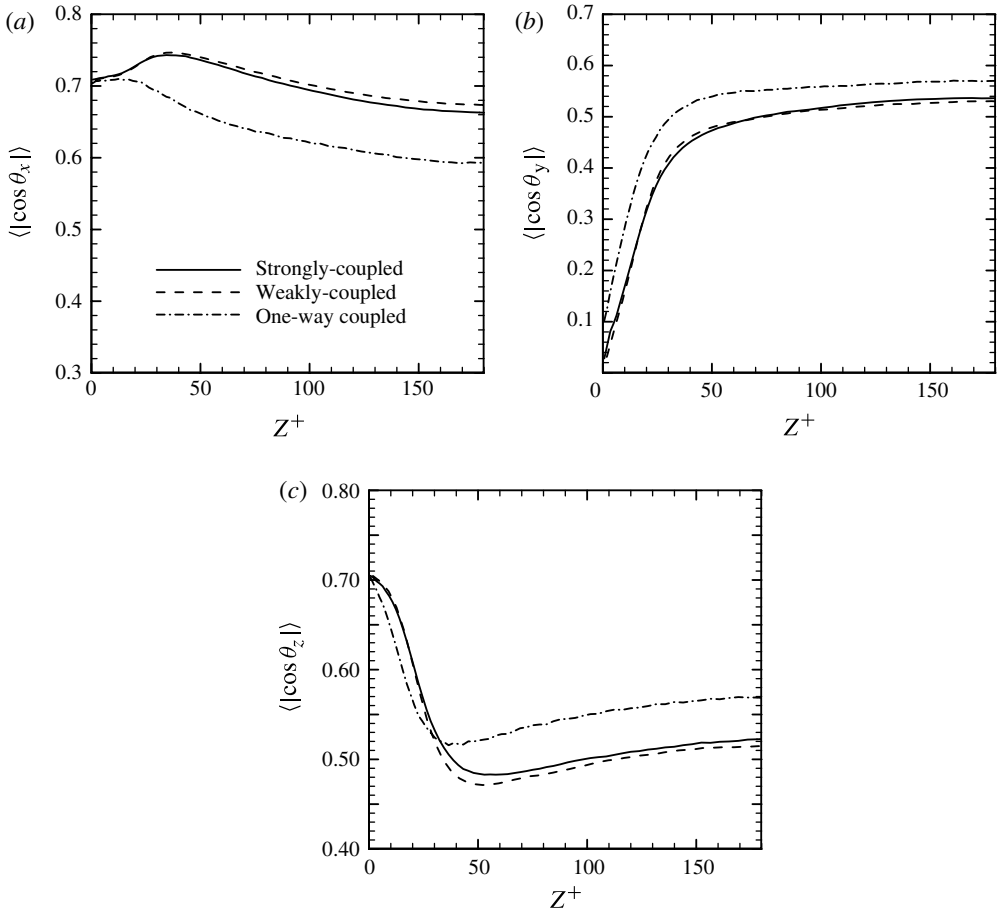

FIGURE 3. Mean particle orientation in the weakly- and strongly-coupled simulations: (*a*) Streamwise direction cosine $|\cos\theta_x|$; (*b*) spanwise direction cosine $|\cos\theta_y|$; (*c*) wall-normal direction cosine $|\cos\theta_z|$. Legend as in figure 2.

and torque-coupled simulation, except that the shear stress $\langle u_x' u_z' \rangle$ being further damped by the inclusion of torque-coupling.

The orientation of non-spherical particles is determined by the turbulence of the carrier fluid and will thus be affected by the modulation of the flow field caused by the feedback from the particles onto the fluid. The instantaneous orientation of the semi-major axis of a given spheroid relative to the coordinate axes $x_i = \langle x, y, z \rangle$ of the inertial frame is defined by means of the direction angles $\theta_i = \langle \theta_x, \theta_y, \theta_z \rangle$. Mean values of the direction cosines $|\cos\theta_i|$ are presented in figure 3. The variation of the direction cosines in the one-way coupled case exhibits the same trends as reported by Mortensen *et al.* (2008) for ellipsoidal particles with somewhat different aspect ratios but the same response time $\tau^+ = 30$. However, the tendency of the elongated particles to align themselves in the mean flow direction is more pronounced in the two-way coupled simulations. Mortensen *et al.* (2008) speculated that the preferential orientation in the streamwise direction was caused by the intense fluctuations of the streamwise fluid velocity. According to the data in figure 2(*b*), a major effect of the feedback from the point particles on the fluid is a further increase of streamwise

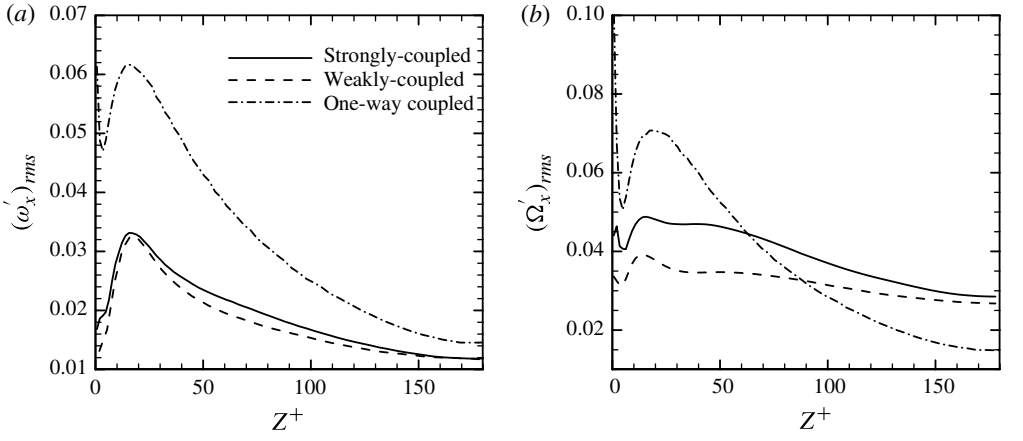

FIGURE 4. The streamwise component of the fluctuating spin vector. (*a*) particle spin $(\omega_x')_{rms}$; (*b*) fluid spin $(\Omega_x')_{rms}$. Legend as in figure 2.

fluctuations. Indeed, the $|\cos\theta_x|$-profile in figure 3(*a*) exhibits a distinct peak around $z^+ \approx 30$, i.e. fairly close to where the streamwise velocity fluctuations are most intense. The partial alignment of the particles with the x-direction becomes somewhat reduced when torque-coupling is also included together with force-coupling and this is thus consistent with the slightly reduced turbulence intensity $(u_x')_{rms}$. According to the data in figure 2, the point particles impart a larger anisotropy to the fluid velocity fluctuations than that observed in the one-way coupled case. This explains why the almost isotropic particle orientation in the channel centre becomes distinctly anisotropic in the weakly- and strongly-coupled simulations.

The fluctuating part of the streamwise angular velocity of the fluid and particles is shown in figure 4. In the one-way coupled simulation the fluctuating particle spin $(\omega_x')_{rms}$ exhibits almost exactly the same variation across the channel as the fluid spin $(\Omega_x')_{rms}$ where the local maximum around $z^+ = 20$ is a signature of the coherent vortices which represent a dominating agent in near-wall turbulence. The streamwise fluid vorticity is substantially reduced in the near-wall region and increased in the core region in the two-way coupled simulations, whereas the corresponding particle spin is damped all across the channel. It is noteworthy that inclusion of torque-coupling in addition to force-coupling has an almost negligible effect on the particle spin intensity in figure 4(*a*), whereas torque-coupling tends to oppose the tendency of two-way force-coupling to damp the coherent vortices (Zhao *et al.* 2010). The distinctly higher fluid spin intensity in figure 4(*b*) than particle spin intensity in figure 4(*a*) suggests that the inertial particles are either unable to adjust to the local fluid rotation or tend to avoid regions with locally high streamwise vorticity.

The three components of the mean particle force f_i^P defined in (2.7) and the non-zero elements of the mean particle stress tensor T_{ij}^P defined in (2.9) are shown in figure 5. The spanwise component of the former and $\langle T_{23}^P \rangle$ are practically zero. This is in accordance with the symmetries of the present flow and therefore reflects the adequacy of the sampling time. The mean value of the streamwise force $\langle f_x^P \rangle$ in the particle-laden momentum equation (2.5) is positive in the near-wall region and becomes negative throughout the logarithmic region and all the way to the channel centre. It is readily seen from figure 1(*a*) that the positive contributions to $\langle f_x^P \rangle$ are

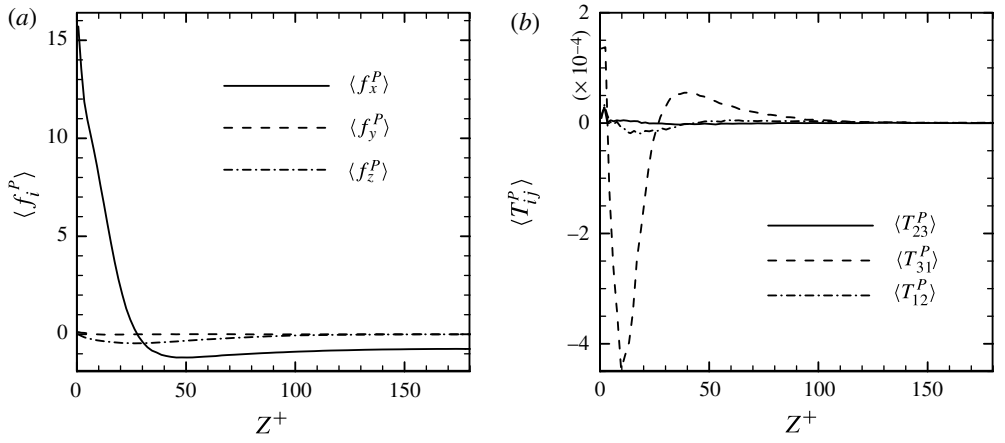

FIGURE 5. Mean values of the particle force (2.7) and the particle stress (2.9). (*a*) mean particle force $\langle f_i^P \rangle$; (*b*) mean particle stress $\langle T_{ij}^P \rangle$.

confined to $z^+ < 20$ and are, moreover, evenly distributed in the spanwise direction, whereas the negative contributions, i.e. regions where the fluid moves faster than the particles, stem from certain localized areas, e.g. around $Y = 2.3$ in figure 1(*a*). The non-zero elements of the mean particle stress tensor T_{ij}^P are shown in figure 5(*b*). The only significant element is $T_{31}^P = -T_{13}^P = (1/\Delta)\sum_{l=1}^{n_p} N_2$ which exhibits an abrupt variation in the viscous-affected near-wall region. After time-averaging this gives rise to the new term $\mathrm{d}\langle T_{31}^P \rangle / \mathrm{d}x_3$ in the Reynolds-averaged Cauchy equation (2.5), which inevitably changes sign where $\langle T_{31}^P \rangle$ attains its minimum value close to $z^+ = 10$. The distribution of $\langle T_{31}^P \rangle$ suggests that the torque-coupling is influential only in the viscous sublayer and the buffer region.

4. Concluding remarks

We have devised a torque-coupling scheme for point particles which enables a stronger mechanical coupling between the Lagrangian particulate phase and the Eulerian fluid phase than a standard two-way coupling scheme. A particle stress tensor expressed in terms of the relative angular velocity, i.e. the spin-slip, was included in the Cauchy equation which governed the carrier-phase turbulence. The inclusion of torque-coupling in addition to force-coupling represents a refinement of earlier two-way coupled simulations.

A strongly-coupled simulation with 2.5 million spheroidal particles with aspect ratio 5 was performed to demonstrate the impact of strong coupling between the particles and the fluid. The results obtained with both force- and torque-coupling (i.e. strong coupling) were compared with data from a two-way coupled simulation, i.e. only force-coupled and thus weak coupling. Force-coupling alone has a major effect on the flow field and the observed modulations of the turbulence resemble those observed for spherical particles by Zhao *et al.* (2010). Inclusion of torque-coupling tends to oppose the effect of force-coupling. Although the resulting torque force in the Cauchy equation attains appreciable values only in the viscous and buffer sublayers, the flow field and the particle orientations are affected all the way to the channel centre.

Acknowledgements

This work has been supported by The Research Council of Norway (project no. 191210/V30) and A/S Norske Shell (contract no. 4610020178/C08156) through research fellowships to M.B. and L.Z. and by The Research Council of Norway (Programme for Supercomputing) through a grant of computing time.

REFERENCES

BALACHANDAR, S. & EATON, J. K. 2010 Turbulent dispersed multiphase flow. *Annu. Rev. Fluid Mech.* **42**, 111–133.

BRENNER, H. 1964 The Stokes resistance of an arbitrary particle IV. Arbitrary fields of flow. *Chem. Engng Sci.* **19**, 703–727.

EATON, J. K. 2009 Two-way coupled turbulence simulations of gas-particle flows using point-particle tracking. *Intl J. Multiphase Flow* **35**, 792–800.

ERINGEN, A. C. 1966 Theory of micropolar fluids. *J. Math. Mech.* **16**, 1–18.

HARPER, E. Y. & CHANG, I.-D. 1968 Maximum dissipation resulting from lift in a slow viscous shear flow. *J. Fluid Mech.* **33**, 209–225.

IRGENS, F. 2008 *Continuum Mechanics*. Springer.

JEFFERY, G. B. 1922 The motion of ellipsoidal particles immersed in a viscous fluid. *Proc. R. Soc. Lond.* A **102**, 161–179.

LUCCI, F., FERRANTE, A. & ELGHOBASHI, S. 2010 Modulation of isotropic turbulence by particles of Taylor-length scale size. *J. Fluid Mech.* **650**, 5–55.

ŁUKASZEWICZ, G. 1999 *Micropolar Fluids - Theory and Applications*. Birkhäuser.

MARCHIOLI, C., FANTONI, M. & SOLDATI, A. 2010 Orientation, distribution, and deposition of elongated, inertial fibers in turbulent channel flow. *Phys. Fluids* **22**, 033301.

MORTENSEN, P. H., ANDERSSON, H. I., GILLISSEN, J. J. J. & BOERSMA, B. J. 2008 Dynamics of prolate ellipsoidal particles in a turbulent channel flow. *Phys. Fluids* **20**, 093302.

SQUIRES, K. D. & EATON, J. K. 1990 Particle response and turbulence modification in isotropic turbulence. *Phys. Fluids* A **2**, 1191–1203.

UHLMANN, M. 2008 Interface-resolved direct numerical simulation of vertical particulate channel flow in the turbulent regime. *Phys. Fluids* **20**, 053305.

ZHANG, H., AHMADI, G., FAN, F. G. & MCLAUGHLIN, J. B. 2001 Ellipsoidal particles transport and deposition in turbulent channel flows. *Intl J. Multiphase Flow* **27**, 971–1009.

ZHAO, L. H., ANDERSSON, H. I. & GILLISSEN, J. J. J. 2010 Turbulence modulation and drag reduction by spherical particles. *Phys. Fluids* **22**, 081702.

ZHAO, L. H. & ANDERSSON, H. I. 2011 On particle spin in two-way coupled turbulent channel flow simulations. *Phys. Fluids* **23**, 093302.